



Published in final edited form as:

Arterioscler Thromb Vasc Biol. 2019 May ; 39(5): 876–887. doi:10.1161/ATVBAHA.119.312434.

Smooth Muscle Cells Contribute the Majority of Foam Cells in Apolipoprotein E-Deficient Mouse Atherosclerosis

Ying Wang, PhD^{1,2}, Joshua A. Dubland, PhD¹, Sima Allahverdian, MD, PhD¹, Enyinnaya Asonye¹, Basak Sahin, MS¹, Jen Erh Jaw, PhD¹, Don D. Sin, MD¹, Michael A. Seidman, MD³, Nicholas J. Leeper, MD², and Gordon A. Francis, MD¹

¹Department of Medicine, Centre for Heart Lung Innovation, Providence Healthcare Research Institute, St. Paul's Hospital, University of British Columbia, Vancouver, British Columbia, Canada

²Division of Vascular Surgery, Stanford University, Stanford, California, United States

³Department of Pathology and Laboratory Medicine, Centre for Heart Lung Innovation, Providence Healthcare Research Institute, St. Paul's Hospital, University of British Columbia, Vancouver, British Columbia, Canada

Abstract

Objective: Smooth muscle cells (SMCs) are the most abundant cells in human atherosclerotic lesions and are suggested to contribute at least 50% of atheroma foam cells. In mice, SMCs contribute fewer total lesional cells. The purpose of this study was to determine the contribution of SMCs to total foam cells in ApoE^{-/-} mice, and the utility of these mice to model human SMC foam cell biology and interventions.

Approach and Results: Using flow cytometry, foam cells in the aortic arch of ApoE^{-/-} mice were characterized based on expression of leukocyte-specific markers. Non-leukocyte foam cells increased from 37% of total foam cells in 27-week-old to 75% in 57-week-old male ApoE^{-/-} mice fed a chow diet, and were approximately 70% in male and female ApoE^{-/-} mice following 6 weeks of Western diet (WD) feeding. A similar contribution to total foam cells by SMCs was found using SMC-lineage tracing ApoE^{-/-} mice fed the WD for 6 or 12 weeks. Non-leukocyte foam cells contributed a similar percentage of total atheroma cholesterol, and exhibited lower expression of the cholesterol exporter ATP-binding cassette transporter A1 (ABCA1) when compared to leukocyte-derived foam cells.

Conclusions: Consistent with previous studies of human atheromas, we present evidence that SMCs contribute the majority of atheroma foam cells in ApoE^{-/-} mice fed a WD and a chow diet for longer periods. Reduced expression of ABCA1, also seen in human intimal SMCs, suggests a common mechanism for formation of SMC foam cells across species, and represents a novel target to enhance atherosclerosis regression.

Correspondence to: Gordon A. Francis, St. Paul's Hospital, Room 166 - 1081 Burrard Street, Vancouver, BC V6Z 1Y6, Phone Number: 1-(604) 806-9269, Fax Number: 1-(604) 806-9274, gordon.francis@hli.ubc.ca.

^c)Disclosures: None

Keywords

atherosclerosis; cholesterol efflux; foam cells; leukocytes; macrophages; smooth muscle cells; Animal Models of Human Disease; Atherosclerosis; Lipids and Cholesterol; Vascular Biology

Introduction

Retention of lipoprotein cholesterol in artery walls is considered the key driver of atherosclerotic plaque formation¹, and removal of this cholesterol is a requirement for plaque regression². In the last 25 years studies of arterial cholesterol metabolism have focused primarily on mouse models, and on the role of monocyte-derived macrophages in taking up excess cholesterol and driving plaque formation, inflammation and progression³. Macrophages have been called the most abundant cell type in mouse atherosclerotic plaque⁴, and inhibition of initial monocyte recruitment into the mouse artery wall can nearly abolish plaque development^{5, 6}.

In contrast to mice and most animal models of atherosclerosis⁷, humans develop a thick layer of smooth muscle cells (SMCs) in the intima known as diffuse intimal thickening (DIT) beginning *in utero* in atherosclerosis-prone arteries⁸. Proteoglycans secreted by DIT SMCs promote the initial retention of apolipoprotein B-containing lipoproteins predominantly in the deep intima, away from macrophages that accumulate initially in the immediate subendothelial space⁹. Autopsy studies of young adults in the 1980's suggested SMCs are a major contributor to cholesterol-overloaded foam cells in early stages of atherosclerosis¹⁰. We previously presented evidence suggesting at least 50% of foam cells in human coronary artery atheromas are SMC-derived¹¹. We also found that SMCs in human coronary intima have reduced expression of the rate-limiting promoter of cholesterol efflux, ATP-binding cassette transporter A1 (ABCA1), when compared to intimal leukocytes¹¹. Lower ABCA1 expression suggests a potential reason for SMCs to become foam cells, and that SMC foam cells in plaque may be resistant to cholesterol efflux-dependent regression when compared to macrophage foam cells¹².

The relative contribution of SMCs to total foam cells in mouse atherosclerosis has not previously been determined. Such analysis has been difficult due to the fact that arterial intimal SMCs frequently express macrophage markers. Upon cholesterol loading cultured mouse arterial SMCs show decreased expression of classic SMC markers such as SM α -actin (SMA) and myosin heavy chain and increased expression of macrophage markers including CD68 and Mac-2¹³. Feil *et al.* reported expression of macrophage markers by intimal SMCs in mice, and that a high number of intimal SMCs take up oxidized LDL, but did not quantitate the relative contribution of SMCs and macrophages to the total foam cell population¹⁴. Further studies from the Owens group, using ApoE-deficient mice expressing a SMC-lineage tracing marker, estimated that more than 80% of intimal SMCs lack classic SMC markers¹⁵. Unlike human arterial intima where up to 90% of cells may be SMCs¹⁶, these studies estimated SMCs constitute approximately 36% of total cells in advanced mouse plaque, but also did not quantitate the contribution of SMCs to foam cells.

The much lower contribution of SMCs to total intimal cells in mice compared to humans, absence of DIT in mice, and the previously documented numeric and functional importance of macrophages in mouse atherosclerosis led us to hypothesize that macrophages would comprise the majority of foam cells in ApoE-deficient mice. This could potentially represent a fundamental limitation in the use of mice to understand human SMC foam cell biology. In the current studies we used a flow cytometry method to investigate the contribution of SMC foam cells to the total foam cell population in ApoE-deficient mice fed a chow diet for 27 and 57 weeks or a Western diet (WD) for 6 or 12 weeks, and the relative expression of ABCA1 by leukocyte- and non-leukocyte-derived foam cells. Contrary to our expectation, our data using both SMC non-lineage-tracing and lineage-tracing mice suggest SMCs contribute the majority of total foam cells in both WD- and older chow-fed ApoE-deficient mice. Similar to human intimal SMCs, we also found reduced expression of ABCA1 in SMC-derived compared to macrophage-derived foam cells in these mice.

Materials and Methods

The data that support the findings of this study are available from the corresponding author upon reasonable request.

The authors declare that all supporting data are available within the article and its online-only Data Supplement or from the corresponding author upon request. Additional Methods are available in the online-only Data Supplement.

Animal procedures.

8-week-old male and female ApoE^{-/-} mice on a C57BL/6 background (Jackson Laboratory) were fed a Western diet (WD, 21% fat, 0.2% cholesterol, Harland Teklad) for 6 weeks to generate early to intermediate lesions without foam cell apoptosis or necrosis. To study spontaneous atherosclerosis, male ApoE^{-/-} mice were fed a chow diet until sacrifice at 27, 36 and 57 weeks. Aortas were collected from the base of the aorta at the aortic valve up to the diaphragm, and adventitia and surrounding adipose tissue were removed. For immunostaining experiments aortic roots were cut from the atria to the apex of the heart and frozen in OCT, except for those from 36-week-old chow-fed mice which were fixed in 10% neutral buffered formalin for later lipid fixation studies. The remaining aortas were cut into 2 sections, one containing the ascending aorta and aortic arch (lesion-prone) and the other the descending aorta (lesion-resistant) for flow cytometry. Small sections of both aortic segments were collected for histology studies. All procedures were performed in accordance with guidelines of the Canadian Council on Animal Care and were approved by the University of British Columbia Animal Care Committee. Male Myh11-Cre^{ERT2}, Rosa26^{Rainbow/+}, ApoE^{-/-} mice (Rainbow mice) and Myh11-Cre^{ERT2}, Rosa26^{tdTomato/tdTomato}, ApoE^{-/-} SMC lineage-tracing mice (Tomato mice) were generated at Stanford University as described in the Online Only Supplemental Methods, using a rainbow reporter as described previously¹⁷ or a Tomato reporter (Jackson Laboratory, B6.Cg-Gt(ROSA)26Sor^{tm14(CAG-tdTomato)Hze/J}). For all studies using SMC-lineage tracing mice, only male animals were available since the Cre allele was initially inserted into the Y chromosome (Jackson Laboratory, B6.FVB-Tg(Myh11-cre/ERT2)1Soff/J).

Immunofluorescence and confocal microscopy.

Serial sections (5 μm) of aortic root beyond the end of the aortic sinus were selected for staining¹⁸. Sections were blocked with 5% goat serum before incubating with rabbit anti-SM α -actin (SMA, Abcam, 0.5 $\mu\text{g}/\text{ml}$) or rat anti-CD45 (BD Pharmingen, 5 $\mu\text{g}/\text{ml}$) primary antibodies. Goat anti-rabbit Alexa fluor595 or goat anti-rabbit Alexa fluor532 were used as secondary antibodies for probing SM α -actin, and goat anti-rat Alexa fluor633 secondary antibody for CD45. Foam cells were stained with 10 $\mu\text{g}/\text{ml}$ BODIPY 493/503 (Invitrogen) at the same time as secondary antibodies. Z-stacked images using 8 planes of the same region were captured using a Leica scanning confocal microscope, and analyzed by Velocity. Formalin-fixed aortic roots were treated using a lipid fixation protocol before being embedded in paraffin¹⁹.

Flow cytometry method validation.

A collagen gel system²⁰ was created to evaluate the effect of the tissue digestion and flow cytometry procedure on foam cell quantitation. To attempt this comparison in tissue, individual lesions were isolated from Tomato SMC lineage-tracing mice, dissected vertically into two parts of similar sizes, and foam cell composition analyzed by flow cytometry and confocal cell counting separately.

Flow cytometry quantification of foam cell composition and ABCA1 expression.

Aortic segments were first fixed in 1% formaldehyde in PBS for 10 min. Fixation was stopped with 125 mmol/L glycine to avoid over cross-linking and allow later ChIP analysis. Tissues were then washed in PBS, cut into 3 mm pieces, and digested with 4 U/ml Liberase TM (Roche), 60 U/ml Hyaluronidase type 1-s, and 60 U/ml DNase I in PBS at 37 °C for 1 h with gentle shaking. After digestion, the cell suspension was passed through a 70 μm cell strainer and spun down at 600g for 5 min to collect the cell pellet for FACS. Cell pellets were resuspended in PBS containing 1% BSA and 0.1% NaN_3 , and incubated with mouse Fc block (BD Pharmingen) for 10 min at 4 °C, and then with 10 $\mu\text{g}/\text{ml}$ BODIPY 493/503 and fluorescence-conjugated antibodies for 30 min at RT. After washing, cells were resuspended in 20 $\mu\text{g}/\text{ml}$ propidium iodide in PBS and sorted within 1 h using a MoFlo® Astrios™ EQ cell sorter (Beckman). BV421 rat anti-mouse CD45, V500 rat anti-mouse I-A/I-E (BD Pharmingen), and Alexa Fluor647 rat anti-mouse ABCA1 (AbD Serotec) antibodies were used according to manufacturer's instructions. Fluorescence minus one (FMO) controls were applied to facilitate gating of CD45 and I-A/I-E, and to make compensations when necessary. BODIPY 493/503 fluorescence intensity of lesion-free descending aortas was used as the negative control to set the gate for foam cells in lesion-prone aortas. Flow cytometry histograms were analyzed using Summit™ (Beckman) to count the number of foam cells and calculate the percentage of leukocyte and non-leukocyte foam cells in the total foam cell population. ABCA1 levels in different cell populations were compared using median fluorescence intensities. Raw data were reconstructed for presentation using FLOWJO® (FlowJo, LLC).

Preparation of LDL.

LDL was isolated from the serum of healthy donors by sequential ultracentrifugation²¹ and was dialyzed at 4°C against phosphate buffered saline pH 7.5. Aggregated LDL (agLDL) was made by vortexing for 1 min²².

Cholesterol mass and efflux assays.

Cholesterol mass in isolated foam cells as determined by mass spectrometry and cholesterol efflux from cultured mouse macrophages and SMCs were determined using established methods as described in the online Data Supplement.^{23–26}

ChIP assay.

For WD-fed ApoE^{-/-} mice, foam cells negative for both CD45 and I-A/I-E, or positive for either leukocyte marker were sorted separately into ChIP lysis buffer. Sorted foam cells from three animals of the same sex were pooled together for microChIP assay, and enrichment level of H3K4me2 at the *MYH11* locus was determined to indicate cells of SMC lineage as described previously²⁷ using a low cell number ChIP kit (Diagenode). The enrichment levels of this epigenetic mark were also determined in cultured mouse aortic SMCs (MASMCs) and RAW 264.7 macrophages.

Statistics.

Results were analyzed by SPSS and Graphpad Prism for statistical significance between treatment groups. Normality of data was determined using a D'Agostino and Pearson omnibus normality test ($\pm=0.05$) and by visual inspection of normality using Q-Q plots. Homogeneity of variance was determined by performing either an *F*-test or a Levene's test. Suitable parametric or nonparametric tests were used as indicated in the figure legends. Data are presented as mean \pm SEM. *P* values <0.05 were considered significant.

Results

Absence of DIT and limitations of histologic lineage-tracing of foam cells in atherosclerotic lesions of ApoE^{-/-} mice.

In human atherosclerosis-prone arteries including coronaries and aorta, DIT composed of SMCs and their secreted proteoglycans forms an intima beginning *in utero*⁸, which frequently exceeds the thickness of the medial SMC layer in adulthood, regardless of the presence of overt atheroma (Figure 1A, upper panel). In ApoE^{-/-} mice there is no DIT layer; six weeks of WD feeding produces foam cell-rich intimal lesions in the aortic roots (Figure 1A, lower panel). Movat's Pentachrome stains smooth muscle cells deep red; the vacuolization in medial layer SMCs may be a response to the metabolic stress of the hyperlipidemia²⁸, but is not due to lipid deposition (see Figure 2A below). To determine the feasibility of quantitating and lineage-tracing foam cells in mouse lesions histologically, we used a lipid preservation technique¹⁹ that previously allowed us to quantitate individual foam cells in human coronary atheromas¹¹. Aortas from 36-week-old ApoE^{-/-} mice fed a chow diet were treated to fix lipids and then incubated with Oil Red O and antibody against SM α -actin (SMA). Figure 1B shows spindle-shaped foam cells in the deep intima

expressing SMA, suggesting they are SMC-derived and still expressing SMC markers. The pan-leukocyte marker CD45 loses antigen immunoreactivity following the lipid fixation process used (data not shown). In addition, even with clear intracellular lipid localization, the tight clustering of foam cells in the mouse intima does not allow accurate counting of individual cells (Figure 1B). Cryostat sections without lipid fixation were then tested to determine their utility for identifying individual foam cells expressing either CD45 or SMA. To allow identification of multiple cell markers simultaneously, in these and subsequent experiments the lipid dye was switched to BODIPY 493/503 (Figure 1C), which has a narrower fluorescence spectrum than Oil Red O. Most CD45⁺ foam cells were identified in the subendothelial portion of the intima (Figure 1C, yellow square), whereas foam cells expressing SMA weakly were seen mainly in the deep intima (Figure 1C, magenta square). A substantial number of BODIPY⁺ foam cells did not express either marker, implying that these may be SMC-derived but have lost classic SMC marker expression. In the absence of lipid fixation, however, it was not possible to determine intracellular versus extracellular lipid among the mass of foam cells in the intimal space, and therefore to quantify individual foam cells (Figure 1C left panel).

Validation of flow cytometry-based isolation and quantification of foam cells.

Based on these difficulties using traditional histologic and confocal microscopy methods, we utilized and tested the validity of tissue digestion and flow cytometry to isolate and characterize the origin of foam cells from mouse atheromas. As traditional macrophage markers such as CD68 are also expressed in intimal SMCs¹⁴, we first identified foam cells based on their lipid levels using BODIPY 493/503. By microscopy, the descending aorta and medial layer of aortic arch showed abundant SMA expression and weak or no BODIPY staining (Figure 2A, left and right panels), while the intima of aortic arches of ApoE^{-/-} mice fed a WD for 6 weeks contained foam cell-rich lesions that stained strongly for BODIPY and weakly for SMA (Figure 2A, right panel). The lower lipid level of cells isolated from lesion-free descending aortas was therefore used to set low and high thresholds of lipid content to identify foam cells (Figure 2B, panels a-d). Cells in the Lipid^{high} gate were enriched approximately 7-fold in cholesterol compared to cells in the Lipid^{low} gate (42.60 ± 18.14 vs. 6.02 ± 1.66 fmol/cell, n=4, p<0.05), validating our positioning of the FACS gating and the designation of Lipid^{high} cells as foam cells (Fig 2B, panel e). While in some mice the clustering of foam cells was not as clear (Fig 2C, panel a), the Lipid^{high} gate was placed in the same position relative to lesion-free descending aorta in all mice to provide a consistent definition and isolation of foam cells in each animal.

A potential concern of this method is that foam cells of either SMC or leukocyte lineage might be more sensitive than the other to the digestion condition and lost during the isolation process. To test the validity of the tissue digestion method, the fidelity of foam cell quantitation following tissue digestion and FACS was tested in a collagen gel model with mouse arterial SMCs (MASMCs) and RAW 264.7 mouse macrophages co-cultured in a collagen sandwich structure²⁰. We found that foam cell composition determined by FACS following digestion of the collagen gel did not differ from results obtained by counting cells in undigested collagen gel sections by microscopy (Supplemental Figure I).

We also validated the use of CD45 as a marker to separate leukocyte-derived from non-leukocyte-derived foam cells. We found no expression of CD45 in cultured MASCs (Supplemental Figure IIA and B) upon lipid loading. However, a reduction of CD45 fluorescence intensity was seen in RAW 264.7 macrophages treated with agLDL (Supplemental Figure IIA), suggesting that macrophages may exhibit reduced CD45 expression upon lipid loading.

70% of foam cells in in early-stage atherosclerotic lesions are non-leukocyte-derived.

Based on the known loss of SMC-specific markers by the majority of mouse intimal SMCs¹⁵, foam cells in lesion-bearing aortas from WD fed mice (Figure 2C, panel a, Lipid^{high}) were analyzed for expression of leukocyte-specific markers. Given the potential down-regulation of surface CD45 in macrophage-derived foam cells, foam cells were also separated based on expression of I-A/I-E, antigen-presenting cell markers that are expressed at a high level in activated leukocytes in atheromas²⁹. Gates Q3 and Q4 and gates Q1 and Q4 were selected to indicate CD45 or I-A/I-E positivity, respectively (Figure 2C panels d and e), using FMO controls (Figure 2C panels a and b). Expression of I-A/I-E by arterial SMCs has not been reported, and we found very few CD45⁻ foam cells exhibiting expression of I-A/I-E (Figure 2C, e Q1). We therefore used the absence of CD45 and I-A/I-E to quantitate non-leukocytes in the foam cell populations (Figure 2C, gate Q2). Gates Q3 and Q4 of Figure 2C (CD45⁺ cells) were combined to quantitate leukocyte-derived foam cells. In the histogram shown in Figure 2C panel e, CD45⁻ cells represented 56.31% and CD45⁺ cells 43.69% of total foam cells. Total foam cell counts for individual mice are indicated in Figure 2D. Based on this method, we determined that in ApoE^{-/-} mice fed a WD for 6 weeks, 69.47±3.20 % (male) and 73.3±2.35 % (female) (n=9 mice of each sex) of the foam cell populations were non-leukocytes, significantly higher than leukocyte-derived foam cells (29.59±2.94% in male and 27.71±3.54% in female mice) ($P<0.01$) (Figure 2E).

Non-leukocyte foam cells in lesions of ApoE^{-/-} mice are primarily of SMC origin.

To determine the contribution of SMCs to the non-leukocyte foam cell population, CD45⁻ (gate Q2) and CD45⁺ (gate Q3+Q4) foam cells were sorted to determine the enrichment level of dimethylation in lysine 4 of histone H3 (H3K4me2) at the *MYH11* locus, a lineage-specific epigenetic marker of SMCs that persists despite their phenotypic changes during atherogenesis²⁷. The SMC-specific marker was highly enriched in CD45⁻ compared to CD45⁺ foam cells ($P<0.01$), with a level in CD45⁻ foam cells from female and male ApoE^{-/-} mice not significantly different from the cultured SMC positive control (Figure 3). This further validates the gating used to isolate CD45⁺ and CD45⁻ foam cells (Figure 2C panels d and e), and suggests that CD45⁻ non-leukocyte foam cells are primarily of SMC origin.

To confirm these data using an alternate approach, we determined the contribution to total atheroma foam cells and expression of CD45 by SMCs using SMC-lineage tracing ApoE^{-/-} mice. One recent publication reported that 2.6% of SMCs express CD45 in a SMC-lineage tracing wild type mouse model³⁰. We determined CD45 expression by arterial SMCs in SMC-lineage tracing ApoE^{-/-} mice fed a WD for 6 weeks. In these mice with arterial SMCs labeled with intrinsic fluorescent proteins, less than 1% of SMCs were positive for CD45 (Supplemental Figure IIIB, Q4 gates). Therefore, under the conditions of these experiments,

CD45 can be assumed to be a leukocyte-specific marker. In these lineage tracing mice, where non-SMCs all express GFP, 63.36±3.02 % of foam cells (SEM, n=5 male mice) expressed neither GFP nor CD45, indicating their origin as SMCs (Supplemental Figure IVB). Using SMC-specific fluorescent protein expression as an alternate approach, 69.98±4.49% of foam cells were estimated to be SMC-derived (Supplemental Figure IVC). These results are consistent with our estimate of the contribution of SMCs to total foam cells using non-lineage tracing ApoE^{-/-} mice (69.47±3.20% in male mice, Figure 2E).

To quantitate the contribution of SMCs to total foam cells following a longer WD feeding period, and to further attempt to compare the extraction efficiency of the tissue digestion method with histologic quantitation of foam cells, we employed a second SMC lineage-tracing model, Tomato mice. While use of these mice allows more definitive identification of SMC location within lesions, lack of cell boundaries and therefore inability to distinguish intracellular from extracellular lipids again precluded counting of individual foam cells in histologic sections (Supplemental Figure VA and VB). The contribution of SMCs following 12 weeks of WD feeding to total foam cells by FACS analysis (67.77 ± 5.47% SMC-derived vs. 32.23 ± 5.47% non-SMC-derived, avg ± SEM, n=3) (Supplemental Figure VC), however, was further consistent with the results obtained using both non-lineage tracing and Rainbow SMC lineage-tracing mice.

Non-leukocyte contribution to total foam cells and cholesterol accumulation in spontaneous atherosclerosis.

Non-leukocyte contribution to total foam cells was also determined in male non-lineage-tracing ApoE^{-/-} mice fed a chow diet to assess early (27 week) and late-stage (57 week) spontaneous atherosclerosis, using the same methods as in WD-fed animals. At age 27 weeks CD45⁻ cells contributed 36.85±5.49% and CD45⁺ cells 62.12±5.44% to total aortic arch foam cells in chow-fed male ApoE^{-/-} mice (Figure 4A). By 57 weeks of age, these percentages changed to 75.47±2.10% CD45⁻ and 22.90±3.69% CD45⁺ foam cells, similar to SMC lineage- and non-lineage-tracing mice fed a WD for 6 or 12 weeks. In foam cells isolated from ApoE^{-/-} mice fed a chow diet for 27 weeks, although CD45⁺ outnumbered CD45⁻ foam cells, the CD45⁻ foam cells contributed a similar level of cholesterol as CD45⁺ foam cells among the total foam cell pool (Figure 4B). These data suggest that as lesions progress in the chow-fed mice, CD45⁻ foam cells become the predominant foam cell type, and contribute an equivalent or higher amount of total foam cell cholesterol burden than CD45⁺ foam cells.

Non-leukocyte foam cells in ApoE^{-/-} mice exhibit reduced ABCA1 expression.

Based on our prior observation that intimal SMCs in human coronary atheromas exhibit reduced ABCA1 expression compared to either medial arterial SMCs³¹ or intimal leukocytes¹¹, we also determined ABCA1 expression in CD45⁻ and CD45⁺ foam cells from ApoE^{-/-} mice. Compared to CD45⁺ leukocyte-derived foam cells, ABCA1 expression was lower in CD45⁻ foam cells from both female and male ApoE^{-/-} mice fed a WD for 6 weeks, and male ApoE^{-/-} mice fed a chow diet for 27 weeks (Figure 5A). Fold change of ABCA1 mRNA was also higher in cultured RAW 264.7 macrophages (4.39±0.14) compared to MAMSCs (2.7±0.13) exposed to agLAL (Figure 5B), which was consistent with reduced

ABCA1 protein level and reduced cholesterol efflux to apoA-I from MASMCs compared to RAW 264.7 macrophages (Figure 5C). These results are consistent with lower ABCA1 expression in CD45⁻ foam cells *in vivo*, and suggest that there is impaired upregulation of ABCA1 expression and therefore cholesterol efflux in response to cholesterol loading in SMC relative to leukocyte foam cells.

Discussion

Current thinking regarding the main cell type of interest and primary site of cholesterol deposition in atherosclerotic plaque, based primarily on studies in mice, has ascribed these roles to macrophages. While we assumed macrophages would contribute the quantitative majority of foam cells in mouse atherosclerosis, in the current studies we provide evidence using both non-lineage- and SMC lineage-tracing models that SMCs contribute the majority of foam cells in apoE^{-/-} mice fed a Western diet for 6 or 12 weeks or a chow diet for longer periods. While contrary to our initial hypothesis, these results are similar to our prior results in human coronary atheromas where we estimated that SMCs contribute, conservatively, at least 50% of total intimal foam cells¹¹. Also consistent with human lesions¹¹, we find that expression of the rate-limiting exporter of excess cell cholesterol, ABCA1, is reduced in CD45⁻ (primarily SMC-derived) compared to CD45⁺ (leukocyte-derived) foam cells. Reduced ABCA1 expression provides a potential reason for the accumulation of SMC-relative to macrophage-derived foam cells, and also suggests SMC foam cells may be more resistant to regression than macrophage foam cells in atherosclerotic lesions.

We initially attempted to quantitate foam cells using a similar histologic approach used in human lesions. Application of this method to mice is limited by a much greater loss of SMC-specific cell markers including ACTA2/SMA in mouse¹⁵ compared to human intimal SMCs¹¹. Utility of the leukocyte-specific marker CD45, as validated in the current studies (Supplemental Figures II, III, and IV), was restricted due to loss of cell CD45 immunoreactivity following the lipid fixation technique we previously adapted to distinguish intracellular from extracellular lipid in human lesions¹⁹. Without lipid fixation, however, intracellular and extracellular lipid deposits cannot be distinguished from one another, making it impossible to accurately count individual foam cells in histologic sections (Figure 1C and Supplemental Figure V). We therefore developed a tissue digestion and flow cytometry protocol to isolate and lineage-trace foam cells from mouse atheromas. Although flow cytometry is an established method to analyze cell populations from digested arteries^{15, 32}, the methods used might preferentially isolate one lineage of foam cells over another. While the limitations of tissue histologic foam cell quantitation preclude direct comparison with FACS analysis, we performed this comparison using a 3D collagen macrophage and SMC co-culture model. We obtained similar quantitation of SMC- and macrophage-foam cells by both methods (Supplemental Figure I). While the collagen gel system does not mimic directly arterial tissue structure, these results suggest that the tissue digestion and FACS-based approach does not preferentially isolate one lineage of foam cell over the other.

In vivo, cholesterol content in the mixed multi-lineage cell populations from digested vessels is heterogeneous, and presented as a continuous spectrum between non-foam cells and foam

cells (Figure 2B and 2C). To isolate foam cells in arterial lesions for lineage analysis, we characterized the lipid content of cells isolated from lesion-bearing aortic arch with lesion-resistant descending aorta. By this technique we were able to set a consistent threshold of lipid content to isolate cholesterol-enriched foam cells based on the level of BODIPY staining, previously used to identify neutral lipid droplets in flow cytometry^{33, 34} (Figure 2B). We found a 7 to 10-fold increase in cholesterol content in cells above (“Lipid^{high}”) relative to below (“Lipid^{low}”) this threshold in aortic arches of both WD- and chow-fed apoE-deficient mice (Figure 2B panel e), validating the definition of these cells as foam cells or non-foam cells, respectively. Recently, Kim *et al.* described a tissue digestion and flow cytometry method similar to ours and reported secondarily that macrophages comprise the majority of foam cells from mouse atheromas³⁵. The major difference of their results and ours is their requirement of a high level of granularity in BODIPY^{high} cells, as measured by side scatter, to define foam cells, whereas we counted all BODIPY^{high} cells among the foam cell population. As shown in Supplemental Figure VI, removal of lower side scatter cells excludes most SMC foam cells, as well as a significant percentage of macrophage foam cells from the total foam cell analysis. While SMC foam cells may exhibit lower granularity than macrophage foam cells, their similarly high BODIPY (Supplemental Figure VI) and cholesterol (Figures 2B panel e and 4B) content indicates they are a foam cell population that must be included in the analysis.

Our results suggesting ~70% of all foam cells in both male and female ApoE^{-/-} mice fed a WD for 6 weeks are non-leukocyte-derived are striking (Figure 2E). The presence of a high level of enrichment of the SMC-specific epigenetic mark in CD45⁻ foam cells (Figure 3), while not quantitative, suggested the majority of these cells are SMC-derived. Using male Rainbow and Tomato SMC lineage-tracing mice, we confirmed a similar percentage of foam cells being SMC-derived (Supplemental Figures IVC and VC). Additionally, ~20% of non-SMC-derived foam cells (GFP⁺) do not express CD45 (Supplemental Figure IVB panel c). Possible contributors to these CD45⁻/GFP⁺ foam cells are leukocyte-derived foam cells that have lost CD45 expression, or other cell types in the plaque including fibroblasts, myofibroblasts, pericytes or endothelial cells. Among these cell types, myofibroblasts isolated from aortic valves can be converted to foam cells *in vitro*³⁶. Stellate pericyte-like cells have also been reported to accumulate lipids in human atherosclerotic lesions³⁷. Overall, our data from SMC lineage-tracing and non-lineage tracing ApoE^{-/-} mice suggest that following 6 or 12 weeks of WD feedings, or from older apoE^{-/-} mice fed a chow diet, 63-70% of foam cells are SMC-derived, with the majority of our data indicating this percentage is ~70%. The similar results using non-lineage- and lineage-tracing mice indicates non-SMC-lineage tracing will remain useful for future studies of SMC foam cell biology, depending on the question being asked.

Our data suggesting the majority of foam cells are SMC-derived was unexpected. First, mice lack the diffuse intimal thickening layer of SMCs present from birth in atherosclerosis-prone arteries in humans⁷. Migration of SMCs is dependent on secretion of cytokines released by endothelial cells following injury induced by the hyperlipidemia, and by monocytes/macrophages that migrate into the intima in the earliest stages of atherogenesis³⁸⁻⁴⁰. Second, SMCs are estimated to comprise only ~36% of total intimal cells in advanced ApoE^{-/-} mouse lesions¹⁵. Our estimate that ~70% of foam cells in these mice are SMC-derived

therefore suggests SMCs are either more predisposed to accumulate cholesterol than macrophages, or less likely to release excess cholesterol once it is deposited in the cells. SMCs express a variety of scavenger receptors including low density lipoprotein-related protein 1 (LRP1) capable of taking up modified lipoproteins¹². In addition to the known capacity of SMCs to take up modified forms of LDL, we demonstrate for the first time that mouse non-leukocyte foam cells, similar to human intimal SMCs¹¹ have reduced expression of ABCA1, the rate-limiting promoter of cholesterol efflux from foam cells⁴¹, when compared to leukocyte-derived foam cells in both WD and chow-fed ApoE^{-/-} mice (Figure 5). Failure to release excess cholesterol via ABCA1 once it is deposited may therefore be the primary reason SMCs become the main lineage of foam cell. In support of this, even at 27 weeks of chow feeding, where CD45⁻ cells make up only 37% of foam cells, they contain almost 50% of the cholesterol in the total foam cell population (Figure 4B), and fail to upregulate ABCA1 as readily as CD45⁺ foam cells (Figure 5A right panel). This suggests SMCs have a defect in the pathway upregulating ABCA1 expression, resulting in them shifting to become the majority of foam cells after 57 weeks of chow diet (Figure 4A right panel).

Upregulation of ABCA1 expression is dependent on upstream processing of lipoproteins and generation of oxysterols from lysosomally-derived cholesterol to activate ABCA1 transcription⁴². While KLF4 has been described as a master regulator of the switch of intimal SMCs from a SMC towards a macrophage-like phenotype in lesions, ABCA1 expression was not found to be a target of KLF4¹⁵. This implies that a defect intrinsic to arterial SMCs, irrespective of their phenotype, may be responsible for their reduced upregulation of ABCA1 in response to lipid loading when compared to leukocytes. This possibility and the relative ability of macrophage and SMC foam cells to release excess cholesterol during regression of atherosclerosis require further investigation.

The results presented here seem counter to previous studies showing that bone marrow-derived leukocytes are the key factor determining the size and cellular content of mouse lesions. In particular, combined inhibition of multiple chemokine pathways in monocyte recruitment reduced lesion size by 90% in ApoE^{-/-} mice⁶. The interfering strategies used in these and many other studies aimed at reducing monocyte infiltration into the plaque, however, may hinder any downstream effects of monocyte recruitment including stimulation of SMC migration from the media into the intima. We observed that formation of MASMC foam cells in the presence of agLDL was enhanced by coculturing with RAW 264.7 macrophages (Supplemental Figure VII). While the mechanism of this remains to be determined, this indicates an additional mechanism, at least in mice, promoting SMC foam cell formation.

Considering the relationship of our findings to previous work allows us to compare and contrast human and mouse atherogenesis. As indicated in the model shown in Figure 6, a key difference is the lack of the SMC DIT layer in mice. In humans, initial lipid deposition occurs around these SMCs deep in the intima and away from macrophages. In mice initial foam cell formation is primarily from macrophages, with SMCs moving into the plaque later under the influence of endothelial cell and leukocyte-secreted cytokines. While some *in vitro* studies indicate SMC migration from the media may occur parallel to lipid loading in mouse lesions⁴³, and medial layer SMC foam cells have been reported in a canine model⁴⁴, we did

not find evidence of lipid accumulation in medial SMCs in aortic arches with early stage lesions in our mice (Figure 2A). Whether formation of SMC foam cells in the medial layer with subsequent migration to the intima can occur requires further investigation. Our model suggests that, following these different initial events in the two species, SMCs are (human) or become (mouse) the predominant cell lineage contributing to total foam cells, due to lack of ABCA1-dependent cholesterol efflux from SMCs in both species.

Not addressed in this study is the relationship of SMC foam cell formation to expansion of specific clones of SMCs in the intima, and whether SMCs continue to proliferate after becoming foam cells. These studies as well as the transferability of the results to other animal models of atherosclerosis require further investigation.

In conclusion, our current and previous results suggest SMCs are the source of the majority of foam cells in both human¹¹ and established mouse atherosclerosis, and that ABCA1 expression is low in intimal SMCs in both species. These findings have major implications for our understanding of atherosclerosis pathogenesis, and suggest SMC foam cells may be resistant to regression. Determining the mechanism of impaired ABCA1 regulation in arterial intimal SMCs will be critical to designing novel treatments to remove the large fraction of excess artery wall cholesterol held in SMC-derived foam cells. Such therapies may be necessary to reduce myocardial infarctions and stroke beyond what current LDL-lowering therapies can achieve.

Supplementary Material

Refer to Web version on PubMed Central for supplementary material.

Acknowledgments

a) Acknowledgment: The authors thank Beth Whalen, Tatjana Bozin, Amrit Samra and Teddy Chan for technical support.

b) Source of Funding: This work was supported by the Heart and Stroke Foundation of Canada and CIHR Project Grant 148883 (to GAF) and NIH grant R35 HL144475 (to NJL). YW is a recipient of the Michael Smith Foundation for Health Research Trainee Award and American Heart Association Postdoctoral Fellowship (18POST34030084). Flow cytometry analysis for SMC-lineage tracing mice was done on instruments in the Stanford Shared FACS Facility using NIH S10 Shared Instrument Grant S10RR027431-01.

Non-standard Abbreviations and Acronyms

ABCA1	ATP-binding cassette transporter A1
AgLDL	aggregated low density lipoprotein
ApoE^{-/-}	apolipoprotein E-deficient
ChIP	chromatin immunoprecipitation
DIT	diffuse intimal thickening
FACS	fluorescence-activated cell sorting
H3K4me2	dimethylation in lysine 4 of histone H3

LDL	low density lipoprotein
SMC	smooth muscle cell
SMA	SMC α -actin
MASMC	mouse aortic smooth muscle cell
WD	Western diet

References

1. Tabas I, Williams KJ, Boren J. Subendothelial lipoprotein retention as the initiating process in atherosclerosis: Update and therapeutic implications. *Circulation*. 2007;116:1832–1844 [PubMed: 17938300]
2. Feig JE. Regression of atherosclerosis: Insights from animal and clinical studies. *Ann Glob Health*. 2014;80:13–23 [PubMed: 24751561]
3. Moore KJ, Sheedy FJ, Fisher EA. Macrophages in atherosclerosis: A dynamic balance. *Nat Rev Immunol*. 2013;13:709–721 [PubMed: 23995626]
4. Legein B, Temmerman L, Biessen EA, Lutgens E. Inflammation and immune system interactions in atherosclerosis. *Cell Mol Life Sci*. 2013;70:3847–3869 [PubMed: 23430000]
5. Gu L, Okada Y, Clinton SK, Gerard C, Sukhova GK, Libby P, Rollins BJ. Absence of monocyte chemoattractant protein-1 reduces atherosclerosis in low density lipoprotein receptor-deficient mice. *Mol Cell*. 1998;2:275–281 [PubMed: 9734366]
6. Combadiere C, Potteaux S, Rodero M, Simon T, Pezard A, Esposito B, Merval R, Proudfoot A, Tedgui A, Mallat Z. Combined inhibition of ccl2, cx3cr1, and ccr5 abrogates ly6c(hi) and ly6c(lo) monocytoysis and almost abolishes atherosclerosis in hypercholesterolemic mice. *Circulation*. 2008;117:1649–1657 [PubMed: 18347211]
7. Nakashima Y, Wight TN, Sueishi K. Early atherosclerosis in humans: Role of diffuse intimal thickening and extracellular matrix proteoglycans. *Cardiovasc Res*. 2008;79:14–23 [PubMed: 18430750]
8. Ikari Y, McManus BM, Kenyon J, Schwartz SM. Neonatal intima formation in the human coronary artery. *Arterioscler Thromb Vasc Biol*. 1999;19:2036–2040 [PubMed: 10479643]
9. Nakashima Y, Fujii H, Sumiyoshi S, Wight TN, Sueishi K. Early human atherosclerosis: Accumulation of lipid and proteoglycans in intimal thickenings followed by macrophage infiltration. *Arterioscler Thromb Vasc Biol*. 2007;27:1159–1165 [PubMed: 17303781]
10. Wissler RW, Vesselinovitch D, Komatsu A. The contribution of studies of atherosclerotic lesions in young people to future research. *Ann N Y Acad Sci*. 1990;598:418–434 [PubMed: 2248455]
11. Allahverdian S, Chehroudi AC, McManus BM, Abraham T, Francis GA. Contribution of intimal smooth muscle cells to cholesterol accumulation and macrophage-like cells in human atherosclerosis. *Circulation*. 2014;129:1551–1559 [PubMed: 24481950]
12. Dubland JA, Francis GA. So much cholesterol: The unrecognized importance of smooth muscle cells in atherosclerotic foam cell formation. *Curr Opin Lipidol*. 2016;27:155–161 [PubMed: 26836481]
13. Rong JX, Shapiro M, Trogan E, Fisher EA. Transdifferentiation of mouse aortic smooth muscle cells to a macrophage-like state after cholesterol loading. *Proc Natl Acad Sci U S A*. 2003;100:13531–13536 [PubMed: 14581613]
14. Feil S, Fehrenbacher B, Lukowski R, Essmann F, Schulze-Osthoff K, Schaller M, Feil R. Transdifferentiation of vascular smooth muscle cells to macrophage-like cells during atherogenesis. *Circ Res*. 2014;115:662–667 [PubMed: 25070003]
15. Shankman LS, Gomez D, Cherepanova OA, Salmon M, Alencar GF, Haskins RM, Swiatlowska P, Newman AA, Greene ES, Straub AC, Isakson B, Randolph GJ, Owens GK. Klf4-dependent phenotypic modulation of smooth muscle cells has a key role in atherosclerotic plaque pathogenesis. *Nat Med*. 2015;21:628–637 [PubMed: 25985364]

16. Orekhov AN, Andreeva ER, Mikhailova IA, Gordon D. Cell proliferation in normal and atherosclerotic human aorta: Proliferative splash in lipid-rich lesions. *Atherosclerosis*. 1998;139:41 [PubMed: 9699890]
17. Rinkevich Y, Lindau P, Ueno H, Longaker MT, Weissman IL. Germ-layer and lineage-restricted stem/progenitors regenerate the mouse digit tip. *Nature*. 2011;476:409–413 [PubMed: 21866153]
18. Paigen B, Morrow A, Holmes PA, Mitchell D, Williams RA. Quantitative assessment of atherosclerotic lesions in mice. *Atherosclerosis*. 1987;68:231–240 [PubMed: 3426656]
19. Tracy RE, Walia P. Lipid fixation for fat staining in paraffin sections applied to lesions of atherosclerosis. *Virchows Arch*. 2004;445:22–26 [PubMed: 15173942]
20. Artym VV, Matsumoto K. Imaging cells in three-dimensional collagen matrix. *Curr Protoc Cell Biol*. 2010;Chapter 10:Unit 10 18 11–20 [PubMed: 20853341]
21. Chung BH, Wilkinson T, Geer JC, Segrest JP. Preparative and quantitative isolation of plasma lipoproteins: Rapid, single discontinuous density gradient ultracentrifugation in a vertical rotor. *J Lipid Res*. 1980;21:284–291 [PubMed: 7381323]
22. Kubo N, Kikuchi J, Furukawa Y, Sakai T, Ohta H, Iwase S, Yamada H, Sakurabayashi I. Regulatory effects of aggregated ldl on apoptosis during foam cell formation of human peripheral blood monocytes. *FEBS Lett*. 1997;409:177–182 [PubMed: 9202141]
23. Hara A, Radin NS. Lipid extraction of tissues with a low-toxicity solvent. *Anal Biochem*. 1978;90:420–426 [PubMed: 727482]
24. Brown MS, Dana SE, Goldstein JL. Receptor-dependent hydrolysis of cholesteryl esters contained in plasma low density lipoprotein. *Proc Natl Acad Sci U S A*. 1975;72:2925–2929 [PubMed: 241998]
25. Folch J, Lees M, Sloane Stanley GH. A simple method for the isolation and purification of total lipides from animal tissues. *J Biol Chem*. 1957;226:497–509 [PubMed: 13428781]
26. Tian Q, Failla ML, Bohn T, Schwartz SJ. High-performance liquid chromatography/atmospheric pressure chemical ionization tandem mass spectrometry determination of cholesterol uptake by caco-2 cells. *Rapid Commun Mass Spectrom*. 2006;20:3056–3060 [PubMed: 16969766]
27. Gomez D, Shankman LS, Nguyen AT, Owens GK. Detection of histone modifications at specific gene loci in single cells in histological sections. *Nat Methods*. 2013;10:171–177 [PubMed: 23314172]
28. Martinet W, Schrijvers DM, Timmermans JP, Bult H. Interactions between cell death induced by statins and 7-ketocholesterol in rabbit aorta smooth muscle cells. *Br J Pharmacol*. 2008;154:1236–1246 [PubMed: 18469840]
29. Galkina E, Kadl A, Sanders J, Varughese D, Sarembock IJ, Ley K. Lymphocyte recruitment into the aortic wall before and during development of atherosclerosis is partially l-selectin dependent. *J Exp Med*. 2006;203:1273–1282 [PubMed: 16682495]
30. Majesky MW, Horita H, Ostriker A, Lu S, Regan JN, Bagchi A, Dong XR, Poczobutt J, Nemenoff RA, Weiser-Evans MC. Differentiated smooth muscle cells generate a subpopulation of resident vascular progenitor cells in the adventitia regulated by klf4. *Circ Res*. 2017;120:296–311 [PubMed: 27834190]
31. Choi HY, Rahmani M, Wong BW, Allahverdian S, McManus BM, Pickering JG, Chan T, Francis GA. Atp-binding cassette transporter a1 expression and apolipoprotein a-i binding are impaired in intima-type arterial smooth muscle cells. *Circulation*. 2009;119:3223–3231 [PubMed: 19528336]
32. Alberts-Grill N, Rezvan A, Son DJ, Qiu H, Kim CW, Kemp ML, Weyand CM, Jo H. Dynamic immune cell accumulation during flow-induced atherogenesis in mouse carotid artery: An expanded flow cytometry method. *Arterioscler Thromb Vasc Biol*. 2012;32:623–632 [PubMed: 22247254]
33. Grandl M, Schmitz G. Fluorescent high-content imaging allows the discrimination and quantitation of e-ldl-induced lipid droplets and ox-ldl-generated phospholipidosis in human macrophages. *Cytometry A*. 2010;77:231–242 [PubMed: 20014301]
34. Velmurugan N, Sung M, Yim SS, Park MS, Yang JW, Jeong KJ. Evaluation of intracellular lipid bodies in chlamydomonas reinhardtii strains by flow cytometry. *Bioresour Technol*. 2013;138:30–37 [PubMed: 23612159]

35. Kim K, Shim D, Lee JS, et al. Transcriptome analysis reveals nonfoamy rather than foamy plaque macrophages are proinflammatory in atherosclerotic murine models. *Circ Res*. 2018;123:1127–1142 [PubMed: 30359200]
36. Syvaranta S, Alanne-Kinnunen M, Oorni K, Oksjoki R, Kupari M, Kovanen PT, Helske-Suihko S. Potential pathological roles for oxidized low-density lipoprotein and scavenger receptors sr-ai, cd36, and lox-1 in aortic valve stenosis. *Atherosclerosis*. 2014;235:398 [PubMed: 24929820]
37. Ivanova EA, Bobryshev YV, Orekhov AN. Intimal pericytes as the second line of immune defence in atherosclerosis. *World J Cardiol*. 2015;7:583–593 [PubMed: 26516412]
38. Paudel KR, Karki R, Kim DW. Cepharanthine inhibits in vitro vsmc proliferation and migration and vascular inflammatory responses mediated by raw264.7. *Toxicol In Vitro*. 2016;34:16–25 [PubMed: 27021874]
39. Koga J, Nakano T, Dahlman JE, Figueiredo JL, Zhang H, Decano J, Khan OF, Niida T, Iwata H, Aster JC, Yagita H, Anderson DG, Ozaki CK, Aikawa M. Macrophage notch ligand delta-like 4 promotes vein graft lesion development: Implications for the treatment of vein graft failure. *Arterioscler Thromb Vasc Biol*. 2015;35:2343–2353 [PubMed: 26404485]
40. Hastings NE, Feaver RE, Lee MY, Wamhoff BR, Blackman BR. Human il-8 regulates smooth muscle cell vcam-1 expression in response to endothelial cells exposed to atheroprone flow. *Arterioscler Thromb Vasc Biol*. 2009;29:725–731 [PubMed: 19229069]
41. Oram JF, Heinecke JW. Atp-binding cassette transporter a1: A cell cholesterol exporter that protects against cardiovascular disease. *Physiol Rev*. 2005;85:1343–1372 [PubMed: 16183915]
42. Pannu PS, Allahverdian S, Francis GA. Oxysterol generation and liver x receptor-dependent reverse cholesterol transport: Not all roads lead to rome. *Mol Cell Endocrinol*. 2013;368:99–107 [PubMed: 22884520]
43. Zhang MJ, Zhou Y, Chen L, Wang X, Pi Y, Long CY, Sun MJ, Chen X, Gao CY, Li JC, Zhang LL. Impaired sirt1 promotes the migration of vascular smooth muscle cell-derived foam cells. *Histochem Cell Biol*. 2016;146:33–43 [PubMed: 26883442]
44. Mahley RW, Innerarity TL, Weisgraber KH, Fry DL. Canine hyperlipoproteinemia and atherosclerosis. Accumulation of lipid by aortic medial cells in vivo and in vitro. *Am J Pathol*. 1977;87:205–226 [PubMed: 192082]

Highlights

- We developed and validated a flow cytometry method to quantitate smooth muscle cell- and leukocyte-derived foam cells in mouse atheromas.
- Smooth muscle cells constitute between 60-70% of total foam cells in both Western Diet- and older chow-fed ApoE^{-/-} mice.
- Mouse SMC foam cells exhibit reduced expression of the rate-limiting exporter of cholesterol ABCA1 when compared to macrophage foam cells.

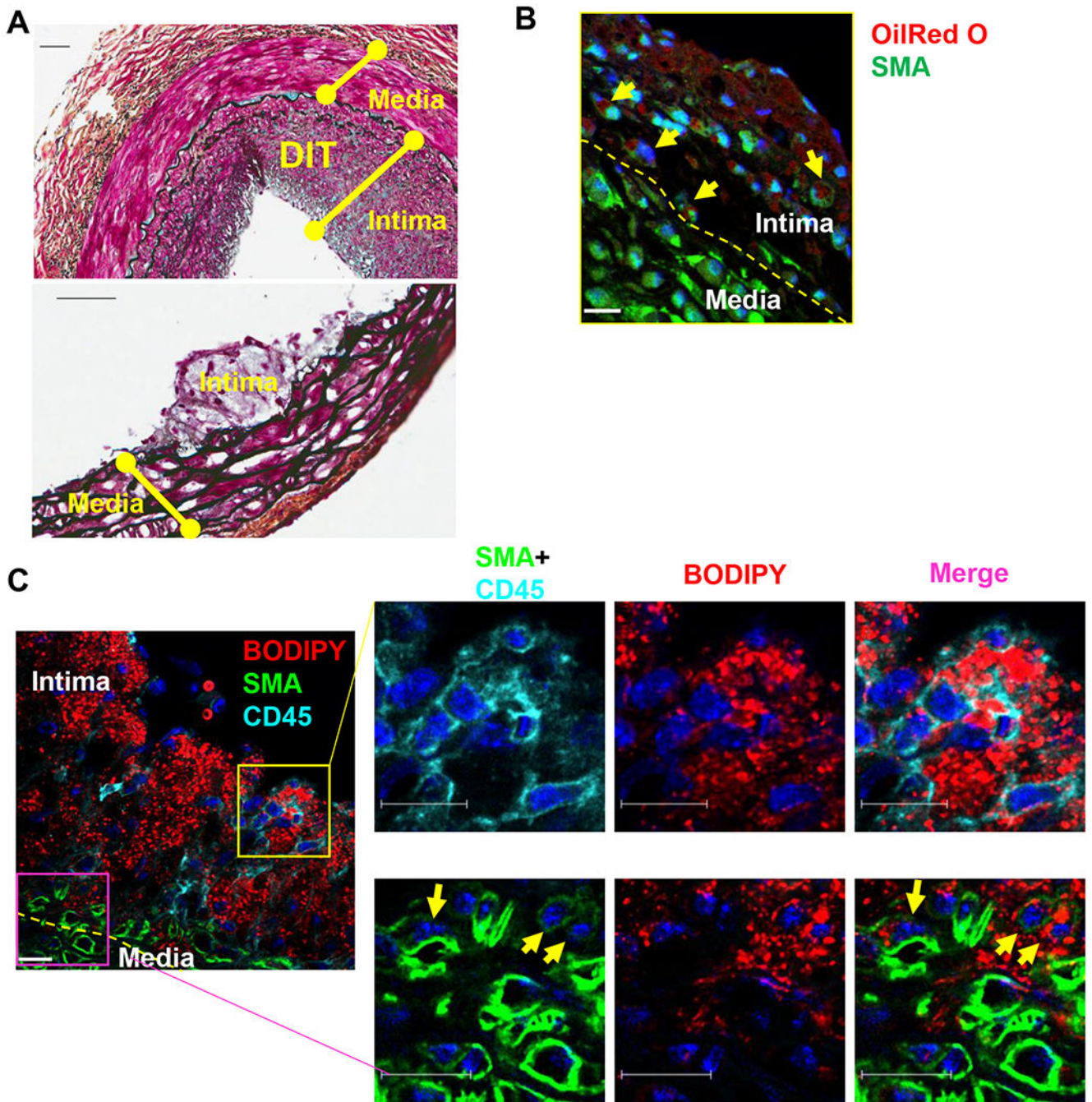


Figure 1. Absence of DIT and challenges quantitating foam cells of specific lineage in the intima of *ApoE*^{-/-} mice by fluorescence microscopy.

(A) Movat's pentachrome stain of a human coronary artery from a 47-year-old male showing typical diffuse intimal thickening (DIT, upper panel), and the aortic root of an 8-week-old *ApoE*^{-/-} mouse fed a WD for 6 weeks showing absence of DIT (lower panel). Scale bar, 50 μ m. (B) Representative fluorescence microscopy of foam cells in the aortic root of a 36-week-old *ApoE*^{-/-} mouse fed a chow diet. Lipid fixation was performed followed by Oil Red O (red) and smooth muscle α -actin (SMA, green) staining. The internal elastic lamina is indicated as a yellow dashed line dividing the intima and media. Yellow

arrows point to foam cells expressing SMA (green). Scale bar, 23 μm . (C) Cryostat section of the aortic root of an 8-week-old male ApoE^{-/-} mouse fed a WD for 6 weeks showing lipid droplets stained by BODIPY (red) and either CD45 (cyan, upper inset boxes) in the proximal intima or SMA (green, lower boxes) in the deep intima. Nuclei were stained by DAPI (blue). Scale bar, 16 μm .

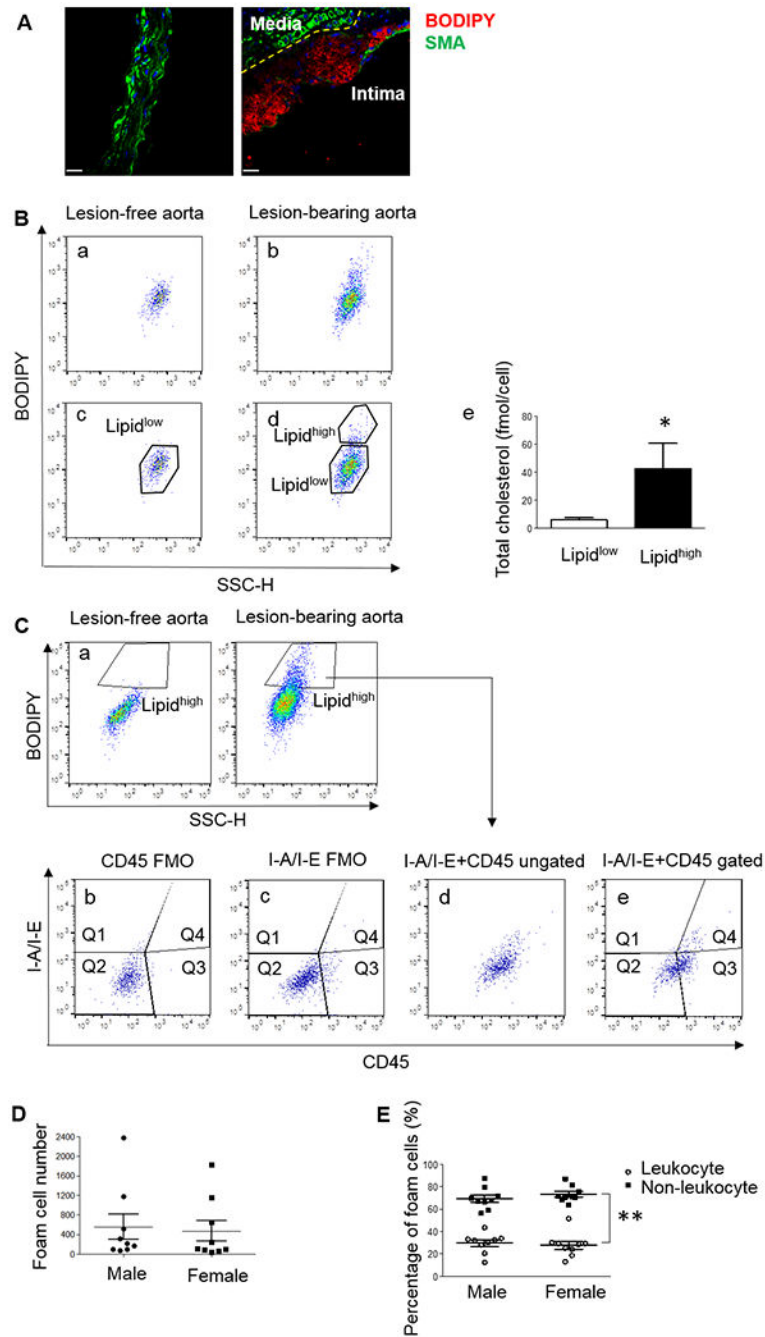


Figure 2. The majority of foam cells in ApoE^{-/-} mice fed a Western diet are non-leukocyte in origin.

(A) Representative immunostaining of lesion-free descending aorta (left panel) and lesion-bearing aortic arch (right panel) of 8-week-old ApoE^{-/-} mice after 6 weeks of WD feeding. Foam cells were labeled with BODIPY (red). The yellow dashed line indicates the internal elastic lamina separating the medial layer exhibiting absence of lipid staining and high levels of SMA (green), and intimal layer containing foam cells (red) and much lower levels of SMA. (B) Histogram identifying foam cells from the aortic arch. Nucleated single events from lesion-bearing aortas (b) have a cell population with higher BODIPY intensity

comparing to lesion-free descending aortas (a). Cells from lesion-free aortas were gated as the Lipid^{low} population (c), and cells above this threshold in atherosclerotic aortic arch were gated as the Lipid^{high} population (d). Cholesterol content in cells in the Lipid^{high} population was much higher than cells in the Lipid^{low} population. N=4 using cells sorted from 4 different animals, * $P < 0.05$ using paired one-sided Student's t test (e). (C) Lipid^{high} cells in the aortic arch of another mouse were identified by comparison to lipid content in lesion-free descending aorta of the same mouse (a), and further separated by their expression of CD45 and I-A/I-E (e). A small aliquot of the same cell suspension was stained in the absence of either CD45 ("fluorescence minus one", FMO, b) or I-A/I-E (c) antibodies as negative controls to set the gates positive for CD45 (Q3 and Q4) and I-A/I-E (Q1 and Q4). Lipid^{high} foam cells were separated by I-A/I-E and CD45 expression at the same time based on the position of the antibody-negative control gates (d and e). (D) Foam cell numbers in the lesion-bearing aortas of individual male and female mice. N=9 mice/group. No statistical differences were found by Mann-Whitney U test between the sexes. (E) Percentage of non-leukocyte foam cells negative for both macrophage markers (Q2) and leukocyte-derived foam cells (Q3+Q4) out of total BODIPY+ events in male and female ApoE^{-/-} mice. N=9 mice/group, ** $P < 0.01$ using 2-way ANOVA with Bonferroni post hoc comparisons.

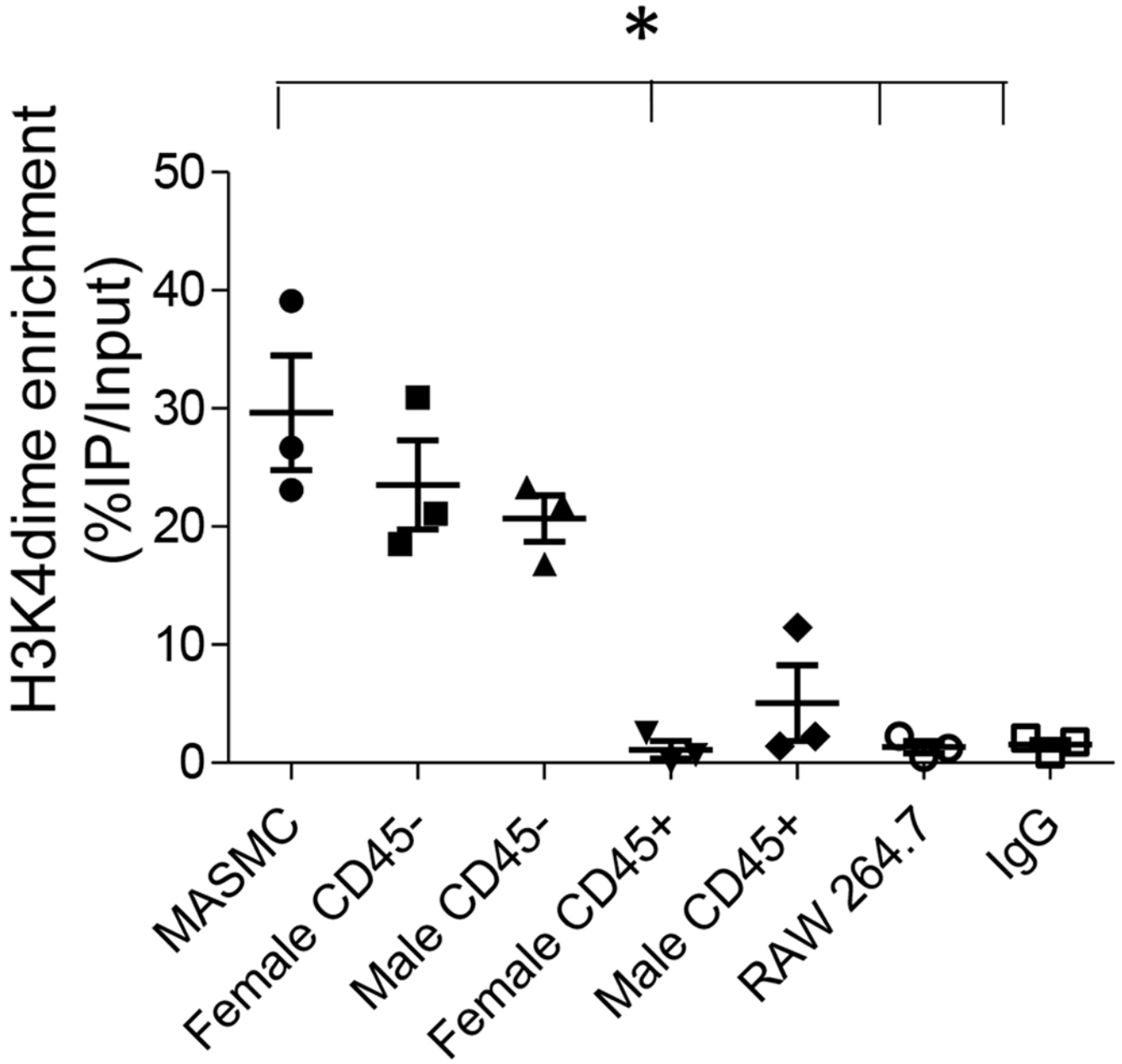


Figure 3. Non-leukocyte foam cells are highly enriched with a SMC-specific epigenetic mark. MicroChIP analysis of enrichment in the SMC-specific lineage mark in CD45⁻ and CD45⁺ foam cells from ApoE^{-/-} mice fed a WD for 6 weeks (isolated in Figure 2C panel e). Cultured MASMCs were measured as positive control. Cultured RAW 264.7 macrophages and sorted CD45⁻ foam cells immunoprecipitated with IgG alone are shown as negative controls. N=3/group, * $P < 0.05$ using Friedman test with Dunn's multiple comparisons versus MASMCs.

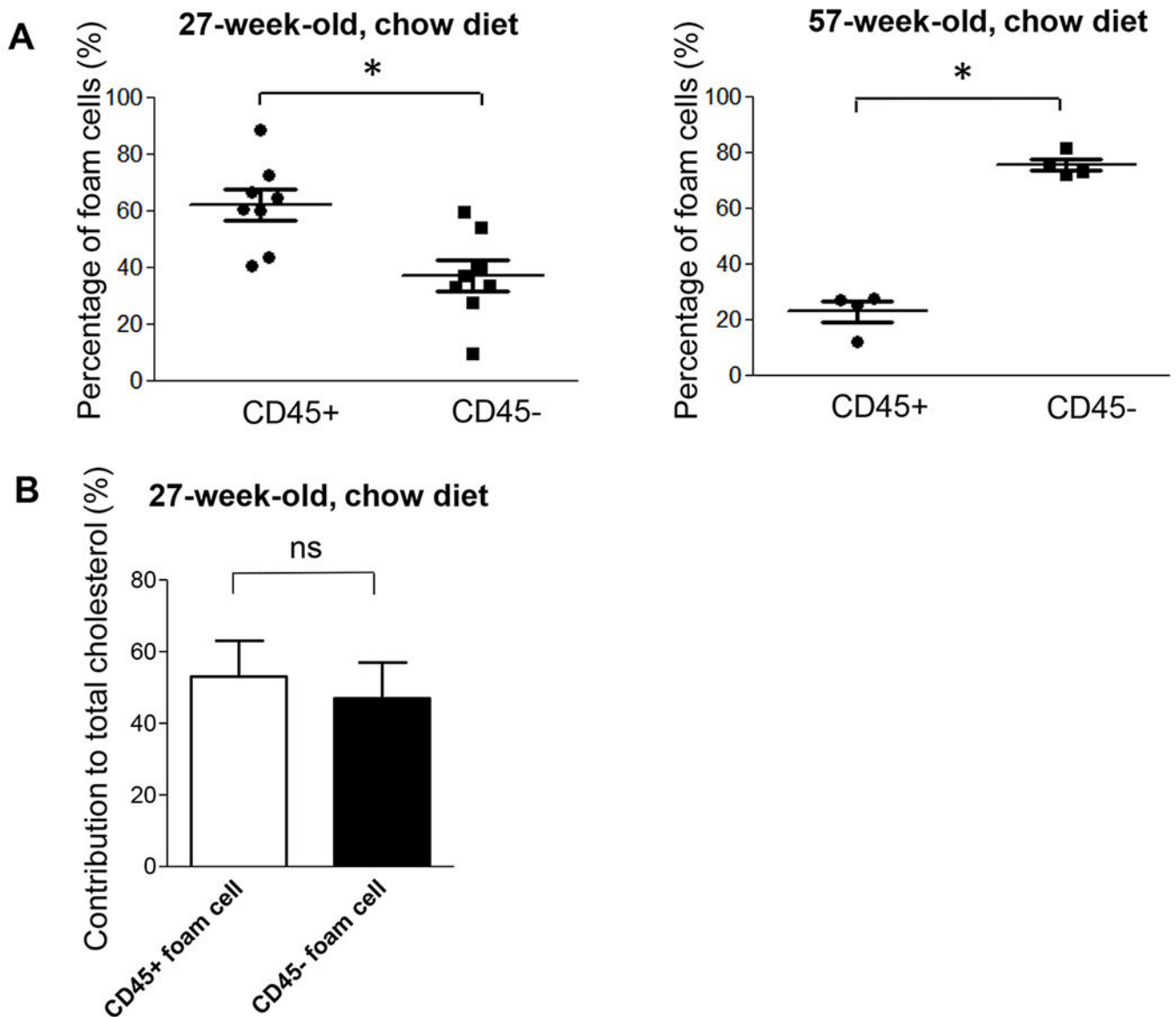


Figure 4. Percentage of non-leukocyte- and leukocyte-derived foam cells in spontaneous atherosclerosis of $ApoE^{-/-}$ mice and their contribution to cholesterol accumulation in arteries. (A) $CD45^{-}$ and $CD45^{+}$ foam cells in the aortic arch were quantified in male 27- (left panel, $n=8$) and 57-week-old (right panel, $n=4$) $ApoE^{-/-}$ mice fed a chow diet. $*P < 0.05$ using a Student's t test (left panel) or Mann-Whitney U test (right panel). (B) $CD45^{+}$ and $CD45^{-}$ foam cells were separated by flow cytometry from 27-week-old mice. Sorted foam cells from 1-3 animals were pooled to obtain sufficient cells for mass determination of cholesterol content ($n=3$ data sets from a total of 8 animals). There was no significant differences in the contribution of $CD45^{+}$ and $CD45^{-}$ foam cells to total cholesterol content in isolated foam cells by Wilcoxon matched pairs sign rank test.

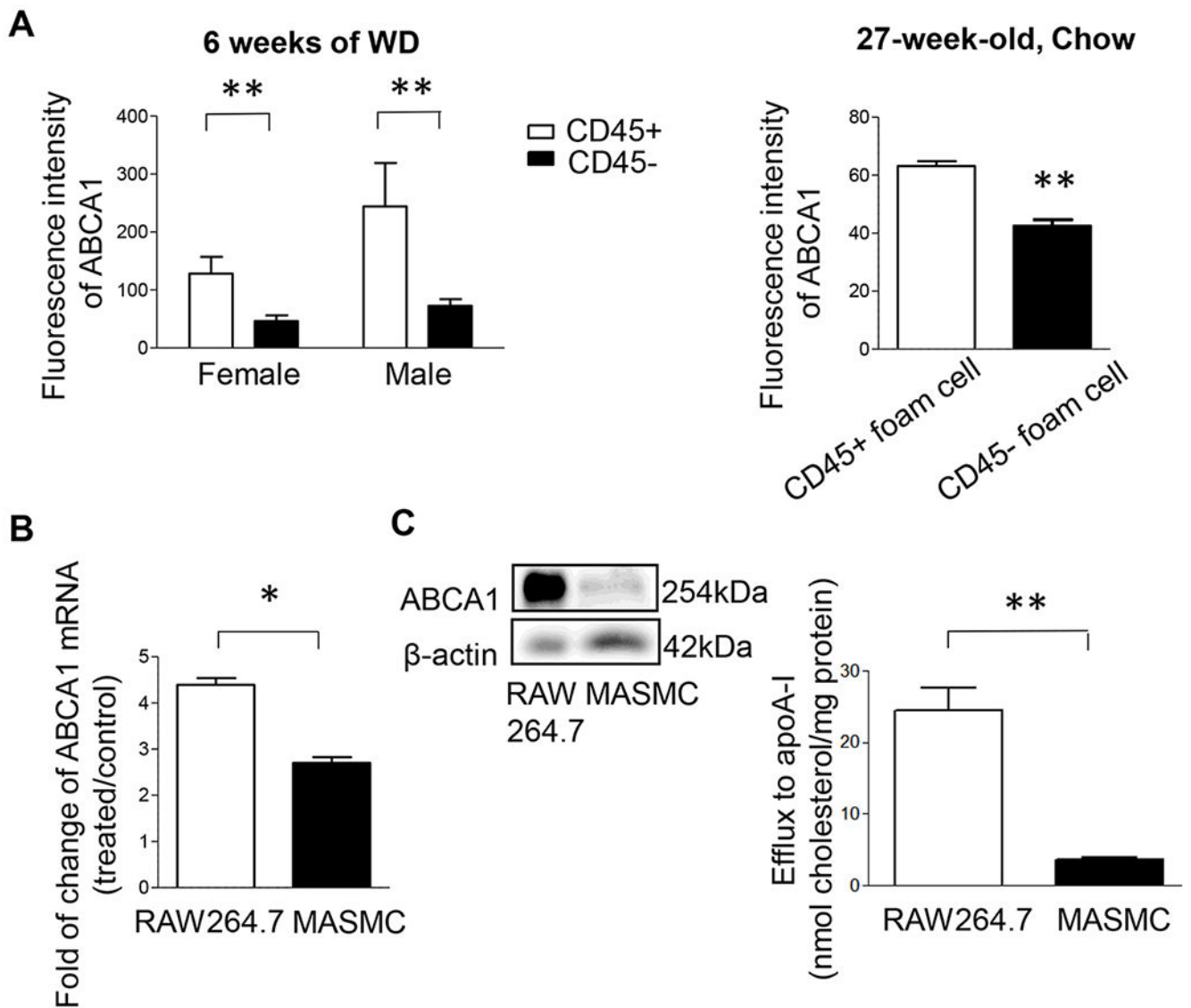


Figure 5. Reduced ABCA1 expression in non-leukocyte foam cells and cultured MAMCs. (A) ABCA1 expression of CD45⁺ and CD45⁻ foam cells from ApoE^{-/-} mice fed a WD for 6 weeks (left panel) or 27-week-old male ApoE^{-/-} mice fed a chow diet (right panel) determined as the median fluorescence of ABCA1 intensity by flow cytometry. For WD-fed mice, ** $P < 0.01$ using two-way ANOVA, $n=9$ mice/group; there was no statistical difference between the two sexes. For chow-fed mice, ** $P < 0.01$ using Mann–Whitney U test, $n=5$ mice/group. (B) Fold change of ABCA1 mRNA level in RAW 264.7 macrophages and MAMCs treated with 100 g/ml agLDL as compared to fatty acid-free albumin alone for 24 h. * $P < 0.05$, using Welch's t test. (C) ABCA1 protein levels and cholesterol efflux from RAW 264.7 macrophages and MAMCs treated with 100 µg/mL agLDL for 48 hrs followed by incubation with 0.3 mM 8Br-cAMP ± 10 µg/mL (for efflux) for 24h. Cholesterol efflux was determined by LC-MS and normalized by total cell protein levels * $P < 0.05$, ** $P < 0.01$ using two-tailed Mann–Whitney U test, $N=5$.

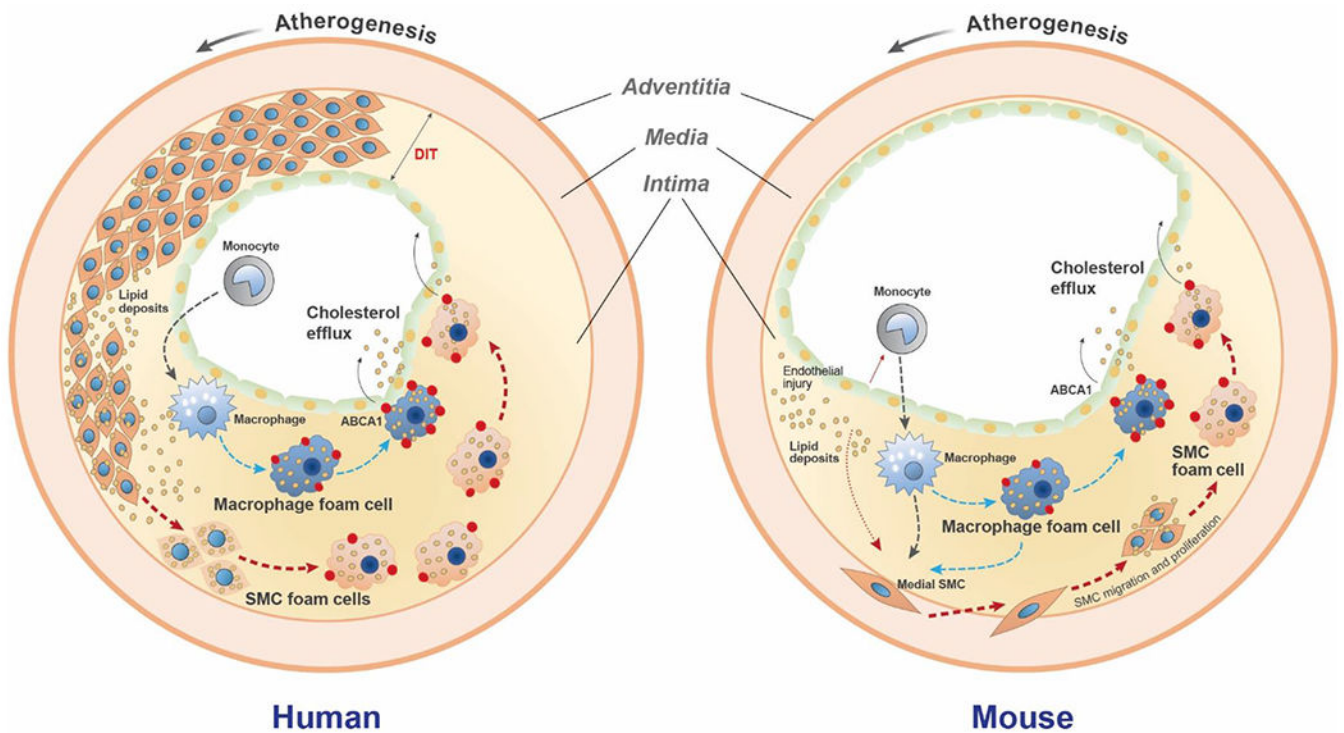


Figure 6. A model comparing early atherogenesis and foam cell formation in humans and ApoE^{-/-} mice.

In humans, a thick diffuse intimal thickening (DIT) layer of SMCs is present in atherosclerosis-prone arteries beginning from birth⁸. At the onset of atherosclerosis lipoproteins that diffuse into the artery wall are trapped through a charge-charge interaction with SMC-secreted proteoglycans, primarily in the deep intima⁷. These trapped lipoproteins are modified and aggregated, becoming a substrate for uptake by the surrounding SMCs. At this stage monocyte/macrophages are located primarily in the subendothelial region away from the deposited lipids⁹. Over time both SMCs and macrophages take up modified lipoproteins to become foam cells independently and/or interactively. ABCA1 (red dots), the rate-limiting cholesterol efflux promoter, is robustly upregulated in macrophage foam cells, but less so in SMC foam cells. Increased ABCA1 expression facilitates cholesterol removal out of macrophage-derived foam cells, while impaired ABCA1 expression reduces cholesterol efflux from SMC foam cells, resulting in SMCs being the predominant lineage among total foam cells. In ApoE^{-/-} mice, no DIT SMC layer is present. Atherogenic lipoproteins induce endothelial injury and monocyte binding and infiltration into the intima, where they mature into macrophages that take up the modified intimal lipids. Cytokines released by injured endothelial cells and monocytes/macrophages, including PDGF, TNF- α , and IL-1 β induce SMC migration from the media into the intima. SMCs proliferate in the intima and take up modified lipoproteins to become foam cells. Similar to human lesions, the SMC foam cells exhibit reduced ABCA1 expression compared to macrophages. Over time the total contribution to foam cells shifts from macrophages to SMCs, due at least in part to impaired ABCA1 expression by the SMC foam cells.